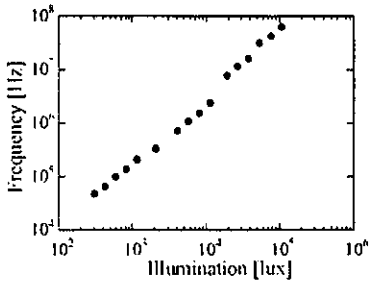

Fig. 11. Experimental results of relationship between incident light intensity and output frequency of PFM photosensor circuit.

3.2. Serial interface circuit

The power consumption of the serial interface circuit was measured using the voltage drop of the off-chip capacitor. A rapid voltage drop of the off-chip capacitor was observed at the rising edge of the recovered clock signal. The observed voltage drop was 1.5 V for a 1000 pF off-chip capacitor with either long or short low pulse duration. This result shows that the rush current of the Schmidt trigger in a clock buffer consumes 300 μW with a data rate of 50 kbit/s, and therefore it dominates the power consumption of the serial interface circuit, while the delay circuit consumes only a few hundred nanowatts.

3.3. PFM pixel circuit

The measured relationship between the incident light intensity and the output frequency of the PFM photosensor at a 5 V supply is shown in Fig. 11. Halogen light was used as a light source. Various neutral density filters were introduced into the light path to give different light intensities. The output frequency is proportional to the incident light intensity over a dynamic range of 60 dB with a high light-to-frequency sensitivity of 190 Hz/lx.

3.4. Current driver circuit

The measured current amplitude from a single device plotted as a function of the DAC digital input code is shown in Fig. 12. The end-point integral nonlinearity (INL) and differential nonlinearity (DNL) errors for the stimulus current were 0.25 LSB and 6.2%, respectively. The output resistance of the current driver was at least 200 kΩ.

The major concern of the current driver circuit is the ability to output an accurate charge-balanced biphasic current pulse. The results show that the current driver circuit is suitable in terms of accuracy, linearity, and output resistance to drive electrode impedance, typically 10 kΩ. Although, as mentioned before, the full-scale current was larger by 30% than the designed value because of the reference current deviation, this did not cause a problem because the external control device compensates for current difference by the configuration data.

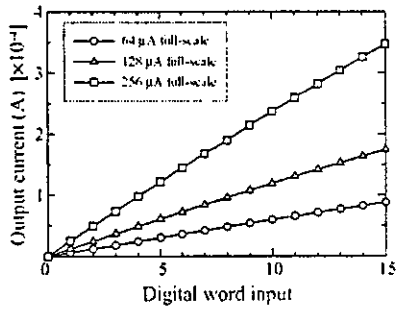

Fig. 12. Experimental results of DAC characteristics with full-scale current amplitude of 64, 128, and 256 μA.

3.5. Operation demonstration

Captured waveforms of the bus signal and stimulus currents are shown in Fig. 13. Three micronodes were connected

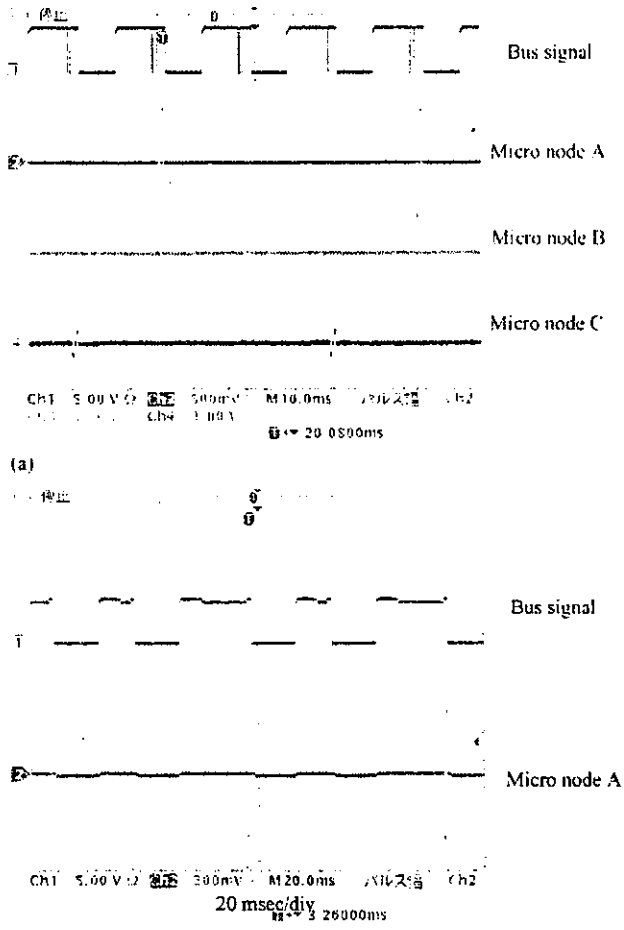

Fig. 13. Captured waveforms of bus signal, stimulus current and internal power voltage. (a) Demonstration of stimulus pulse parameter control over serial link. The horizontal scale is 10 ms/div and the vertical scale of bus signal, micronode A, and micronodes B and C are 5, 0.5, and 1.0 V/div, respectively. (b) Demonstration of image binarization under normal room illumination. The horizontal scale is 20 ms/div and the vertical scale of bus signal and micronode A are 5 and 0.5 V/div, respectively.

to the serial bus. Load resistances of 10 kΩ, which is a typical value of stimulus electrode impedance, were connected to the stimulus electrode of the micronodes. The stimulus current is output only from the addressed micronode and the stimulus pulse width and amplitude are controlled by the packet signal, as shown in Fig. 13(a). The waveform shown in Fig. 13(b) demonstrates image binarization under normal room illumination. The waveform shows that a stimulus current is output in an accumulation time of 20 ms, while it is not output in a time of 5 ms. In other words, the incident light intensity is binarized in a micronode by controlling the accumulation time over the serial bus.

4. Design enhancements

While device operation was demonstrated successfully under normal room light conditions, two improvements of the micronode design should be considered. First, the micronode does not work under extremely strong light, due to reference current circuit malfunction. The photo-induced minority carrier is expected to affect the reference current circuit. This drawback would be overcome by post-process fabrication of optical black on the device. Second, the off-chip capacitance should be eliminated. Although micro-sized 3300 pF capacitors are available, the presence of a capacitor prevents the retinal prosthetic device from achieving high stimulus point density. The off-chip capacitance would be unnecessary if the bus signal amplitude was made very small, for example by changing the present 5–0 V bus signal swing to a 5–4 V swing.

5. Conclusion

A retinal prosthetic device using distributed network-linked micro-sensor architecture is proposed, and the operation of the micronode is demonstrated.

Conventional retinal prosthetic devices, which use polyimide-based flexible stimulus electrode arrays, have problems in the number of stimulus points due to I/O pad restriction. In the proposed device, the stimulus electrodes are replaced with smart micro-sized photo-detecting CMOS devices, known as micronodes. Each micronode directly controls the stimulus currents of the stimulus electrodes. Because micronodes have a serial interface circuit, a single-wire is enough to connect each device so that the device has a maximum number of stimulus points.

The micronode device consists of a single-wire serial interface, a photosensor with pixel-level ADC, an image processing circuit, and a current driver circuit with a current DAC. The micronode is fabricated using 0.6 μm CMOS technology with geometry of 500 μm × 500 μm. The device size is close to the reported spatial resolution of phosphene and indicates that the device is promising for restoring clear vision (Table 1).

Table 1
Characteristics of fabricated device

Device size	500 μm × 500 μm
Operating voltage	2.0–5.0 V
Static current consumption	2.5 μA
Off-chip capacitor	>3000 pF
Dynamic range	>60 dB
Bus speed	50 kbit/s

The prototype device was successfully tested. The stimulus current amplitude and stimulus pulse width were controlled by packet data over the serial bus. Image binarization was demonstrated with a wide dynamic range PFM photosensor coupled with an 8-bit binary counter.

Acknowledgements

This work was supported by the New Energy Development Organization (NEDO) and Health and Labor Sciences Research Grants, Japan. The author would like to thank S. Nishimura and K. Shodo of NIDEK Co. Ltd. for valuable discussions and suggestions.

References

[1] E. Zrenner, Will retinal implants restore vision? Science 295 (2002) 1022–1025.
[2] E. Margalit, M. Maia, J.D. Weiland, R.J. Greenberg, G.Y. Fujii, G. Torres, D.V. Piyathaisere, T.M. O'Hearn, W. Liu, G. Lazzi, G. Dagnelie, D.A. Scribner, E. De Juan Jr., M.S. Humayun, Retinal prosthesis for the blind, Surv. Ophthamol. 47 (2002) 335–356.
[3] M.S. Humayun, E. De Juan Jr., J.D. Weiland, G. Dagnelie, S. Katona, R. Greenberg, S. Suzuki, Pattern electrical stimulation of the human retina, Vis. Res. 39 (1999) 2569–2576.
[4] K. Cha, K.W. Horch, R.A. Normann, Mobility performance with a pixelized vision system, Vis. Res. 32 (1992) 1367–1372.
[5] J. Ohta, N. Yoshida, K. Kagawa, M. Nunoshita, Proposal of application of pulsed vision chip for retinal prosthesis, Jpn. J. Appl. Phys. 1 (41) (2002) 2322–2325.
[6] A. Uehara, K. Kagawa, T. Tokuda, J. Ohta, M. Nunoshita, Back-illuminated pulse-frequency-modulated photosensor using silicon-on-sapphire technology developed for use as epi-retinal prosthesis device, Electron. Lett. 39 (2003) 1102–1104.
[7] A. Uehara, D.C. Ng, K. Kagawa, T. Tokuda, J. Ohta, M. Nunoshita, CMOS retinal prosthesis with on-chip electrode impedance measurement, Electron. Lett. 40 (2004) 582–584.
[8] D.C. Ng, K. Isakari, A. Uehara, K. Kagawa, T. Tokuda, J. Ohta, M. Nunoshita, A study of bending effect on pulse-frequency-modulation-based photosensor for retinal prosthesis, Jpn. J. Appl. Phys. 1 (42) (2003) 7621–7624.
[9] W. Liu, K. Vichienchom, M. Clements, S.C. DeMarco, C. Hughes, E. McGucken, M.S. Humayun, E. De Juan, J.D. Weiland, R. Greenberg, A neuro-stimulus chip with telemetry unit for retinal prosthetic device, IEEE J. Solid State Circuits 35 (2000) 1487–1497.
[10] W. Liu, Retinal implant: bridging engineering and medicine, in: Proceedings of the International Electron Devices Meeting, Technical Digest, 2002, pp. 492–495.
[11] W. Liu, M. Sivaprakasam, P.R. Singh, R. Bashirullah, G. Wang, Electronic visual prosthesis, Artif. Organs. 27 (2003) 986–995.

[12] G.J. Suaning, N.H. Lovell, CMOS neurostimulation ASIC with 100 channels, scaleable output, and bidirectional radio-frequency telemetry, IEEE Trans. Biomed. Eng. 48 (2001) 248–260.
[13] J.U. Meyer, Retina implant-a bioMEMS challenge, Sens. Actuators A 1 (2002) 1–9.
[14] A. Uehara, Y.L. Pan, K. Kagawa, T. Tokuda, J. Ohta, M. Nunoshita, A micro-sized photo detectable stimulator array for retinal prosthesis by distributed sensor network approach, in: Proceedings of the 2003 Symposium on VLSI Circuits, Digest of Technical Papers, 2004, pp. 302–305.
[15] P.J. Rousche, D.S. Pellinen, D.P. Pivin Jr., J.C. Williams, R.J. Vetter, D.R. kirke, Flexible polyimide-based intracortical electrode arrays with bioactive capability, IEEE Trans. Biomed. Eng. 48 (2001) 361–371.
[16] T. Stieglitz, Flexible biomedical microdevices with double-sided electrode arrangements for neural applications, Sens. Actuators A 90 (2001) 203–211.
[17] E. Zrenner, A. Stett, S. Weiss, R.B. Aramant, E. Guenther, K. Kohler, K.-D. Miliczek, M.J. Seiler, H. Haemmerle, Can subretinal microphotodiodes successfully replace degenerated photoreceptors? Vis. Res. 39 (1999) 2555–2567.
[18] A.Y. Chow, M.T. Pardue, V.Y. Chow, G.A. Peyman, C. Liang, J.I. Perlman, N.S. Peachey, Implantation of silicon chip microphotodiode arrays into the cat subretinal space, IEEE Trans. Neural Syst. Rehabil. Eng. 9 (2001) 86–95.
[19] M. Schwarz, L. Ewe, R. Hauschild, B.J. Hosticka, J. Huppertz, S. Kolnsberg, W. Mokwa, H.K. Trieu, Single chip CMOS imagers and flexible microelectronic stimulators for a retina implant system, Sens. Actuators A 83 (2000) 40–46.
[20] D. Ziegler, P. Linderholm, M. Mazza, S. Ferazzutti, D. Bertrand, A.M. Ionescu, Ph. Renaud, An active microphotodiode array of oscillating pixels for retinal stimulation, Sens. Actuators A 110 (2004) 11–17.
[21] A.E. Grumet, J.L. Wyatt Jr., J.F. Rizzo, Multi-electrode stimulation and recording in the isolated retina, J. Neurosci. Meth. 101 (2000) 31–42.
[22] A. Stett, W. Barth, S. Weiss, H. Haemmerle, E. Zrenner, Electrical multisite stimulation of the isolated chicken retina, Vis. Res. 40 (2000) 1785–1795.
[23] C.J. Aswell, J. Berlien, E. Dierschke, M. Hassan, A monolithic light-to-frequency converter with a scalable sensor array, in: Proceedings of the ISSCC Technical Digest, 1994, pp. 158–159.
[24] L.G. McIlrath, A low-power low-noise ultrawide-dynamic range CMOS imager with pixel-parallel A/D conversion, IEEE J. Solid State Circuits 36 (2001) 846–853.
[25] J. Goy, B. Courtois, J.M. Karam, F. Pressecq, Design of an APS CMOS image sensor for low light level applications using standard CMOS technology, Analog Integr. Circuits Signal Process 29 (2001) 95–104.
[26] H.J. Oguey, D. Aebischer, CMOS current reference without resistance, IEEE J. Solid State Circuits 32 (1997) 1132–1135.

Biographies

Akihiro Uehara received the B.S. degree in electrical engineering from Osaka University, Japan in 1997, and M.S. degree from the Nara Institute of Science and Technology, Nara, Japan in 2000. In 2002 he joined the Nidek Vision Institute, Nidek Co., Ltd., Japan, where he has been engaged in the research of artificial vision prosthetic devices. His research interest is in CMOS sensors and mixed-signal circuit design.

Yi-Li Pan received his B.E. degree in Mechanical Engineering from National Sun Yat-Sen University, Taiwan in 1994. He obtained his B.S. degree in Electronic Engineering from University of Warwick, U.K. in 2000. Currently he is a graduate student in the Graduate School of Materials Science of Nara Institute of Science and Technology, Japan. His research is focusing on the studies of retinal prosthesis.

Keiichiro Kagawa received the B.E. degree in applied physics from Osaka University, Japan in 1996. He received the M.E. and Dr. Eng degrees in material and life science in 1998 and 2001, respectively. From 1995 to 2001, he was engaged in research on optical packaging and prototyping of optoelectronic parallel computers. Since 2001, he has been an assistant professor at the Nara Institute of Science and Technology, Nara, Japan. His research interests include CMOS image sensors, vision chips, and optoelectronic systems. Dr. Kagawa is a member of the Japan Society of Applied Physics, the Institute of Image Information and Television Engineers of Japan, and the Institute of Electrical and Electronics Engineers.

Takashi Tokuda received the B.S. and M.S. degrees in electronic engineering from Kyoto University, Kyoto, Japan, in 1993 and 1995, respectively. He received the Dr. Eng. degree in materials engineering from Kyoto University in 1998. He has been an assistant professor in the Graduate School of Materials Science, Nara Institute of Science and Technology, since 1999. He has been working on photonic materials science and photonic device engineering. He is a project member of the development of retinal prostheses devices. His research interests include CMOS image sensors, bio-imaging sensors, and bio-sensing devices.

Jun Ohta was born in Gifu, Japan in 1958. He received the B.E., M.E., and Dr. Eng. degree in applied physics, all from the University of Tokyo, Japan, in 1981, 1983, and 1992, respectively. In 1983, he joined Mitsubishi Electric Corporation, Hyogo, Japan, where he has been engaged in the research on optoelectronic integrated circuits, optical neural networks, and artificial retina chips. From 1992 to 1993, he was a visiting researcher in Optoelectronics Computing Systems Center, University of Colorado at Boulder. In 1998, he has been an Associate Professor in Graduate School of Materials Science, Nara Institute of Science and Technology (NAIST), Nara, Japan, and in 2004, he has been a Professor of NAIST. His current research interests are in vision chips, CMOS image sensors, bio-photonic LSIs, integrated photonic devices. Dr. Ohta received the Best Paper Award of the IEICE Japan in 1992, the Ichimura Award in 1996, and the National Commendation for Invention in 2001. He is a member of the Japan Society of Applied Physics, the Institute of Electronics, Information and Communication Engineers of Japan, the Institute of Image Information and Television Engineers of Japan, the Institute of Electronic and Electronics Engineers, and the Optical Society of America.

Masahiro Nunoshita was born in Okayama, Japan in 1942. He received the B.E., M.E., and Dr. Eng. degrees in electrical engineering, all from Osaka University, Japan, in 1965, 1967 and 1975, respectively. In 1967 he joined the Kyoto works, Mitsubishi Electric Corporation (MELCO), Japan, where he designed color TV sets. In 1969 he was transferred to the Central Research Laboratory, MELCO, Hyogo, Japan, where he studied EL flat panels and amorphous semiconductor devices. Since 1974 he has worked on the R&D of micro-optics and integrated optics for fiber-optic communication and sensing systems and GaAs/AlGaAs opto-electronics. In 1987 he worked as a Project Manager to develop active-matrix and projection-type LCDs, and then joined the project of Si-ULSI technologies. In 1993 he joined the Semiconductor Research Lab., MELCO, where he had directed the R&D of 1Gb-DRAM cells with SR lithography and high-ε capacitors, IR-image sensors with Pt-Si and HgCdTe, blue lasers and LEDs with ZnSe/ZnCdSe and GaN/AlN, and high-Tc superconductive thin-film devices. Since 1998 he has been a Professor in the Graduate School of Materials Science, Nara Institute of Science and Technology, Nara, Japan. Dr. Nunoshita is a member of the Japan Society of Applied Physics, the Institute of Electronics, Information and Communication Engineers of Japan, the American Physical Society, the Optical Society of America and the Institute of Electrical and Electronics Engineers.

(12)

LABORATORY SCIENCES

Histological Effect and Protein Expression in Subthreshold Transpupillary Thermotherapy in Rabbit Eyes

Yoshihiro Morimura, MD; Annabelle A. Okada, MD; Atsushi Hayashi, MD; Sayuri Fujioka, MD; Sumie Kawahara, MD; Tetsuo Hida, MD

Objective: To investigate the histological effect of subthreshold transpupillary thermotherapy (TTT) on the retina.

Methods: We performed TTT in normal pigmented rabbit eyes using an 810-nm diode laser with spot size of 1.2 mm, power of 50 mW, and varying durations of 15, 30, or 60 seconds. Four weeks later, fluorescein angiography was performed, and the enucleated eyes were examined by means of electron microscopy and immunohistochemical staining.

Results: Funduscopy immediately and at 4 weeks showed no discernable changes at TTT sites, and fluorescein angiography at 4 weeks showed no abnormalities. However, electron microscopy showed photoreceptor and retinal pigment epithelium cell disruption, changes more prominent with longer durations of treatment. Immunohistochemical staining was positive for heat shock protein 60, heat shock protein 70, tumor necrosis factor α, and vascular cell adhesion molecule 1 in the photoreceptors and retinal pigment epithelium at TTT sites. Untreated control eyes showed no staining.

Conclusions: Despite the absence of changes evident by funduscopy and fluorescein angiography, TTT resulted in dose-dependent histological changes in photoreceptors and retinal pigment epithelium. The induction of heat shock proteins, cytokines, and cell adhesion molecules may play a role in the tissue response to subthreshold TTT.

Clinical Relevance: Unrecognized damage to the retina and retinal pigment epithelium may contribute to visual loss in eyes that undergo subthreshold TTT.

Arch Ophthalmol. 2004;122:1510-1515

SUBTHRESHOLD TRANSPUPILLARY thermotherapy (TTT) using the 810-nm diode laser represents a method for delivering low-energy, large-spot-size hyperthermia to the retina and choroid. Recently, TTT has been used with some success to reduce exudation associated with subfoveal choroidal neovascularization (CNV) in age-related macular degeneration.[1,2] It has been estimated that the temperature elevation one can expect with subthreshold TTT is 4°C to 10°C.[3,4] However, the exact temperature elevation achieved with such therapy, the influence of various clinical variables on treatment, and dose-dependent histopathological changes that occur with subthreshold TTT are not known. Furthermore, although some researchers have suggested that heat shock protein (HSP) and apoptosis may play a role in the tissue response to TTT,[4,5] the mechanism of action of TTT in eyes with CNV remains largely unknown.

The purpose of this study was to examine the histological effect of TTT in an experimental animal model. We performed subthreshold TTT in normal pigmented rabbit eyes and examined dose-dependent histopathological changes by means of light and electron microscopy. In addition, immunohistochemical staining was performed to investigate expression of HSP60, HSP70, tumor necrosis factor α (TNF-α), and vascular cell adhesion molecule 1 (VCAM-1).

METHODS

ANIMALS

We used rabbits weighing approximately 2 kg with normal pigmented eyes. All animals were housed and experiments were conducted in accordance with the Association for Research in Vision and Ophthalmology Statement on the Use of Animals in Ophthalmic and Vision Research. General anesthesia was induced by intramuscular injection of 30 mg/kg ketamine hydrochloride and 6 mg/kg xylazine hydro-

From the Department of Ophthalmology, Kyorin University School of Medicine, Tokyo, Japan (Drs Morimura, Okada, Kawahara, and Hida); and the Department of Ophthalmology, Osaka University Medical School, Suita, Japan (Drs Hayashi and Fujioka). *The authors have no relevant financial interest in this article.*

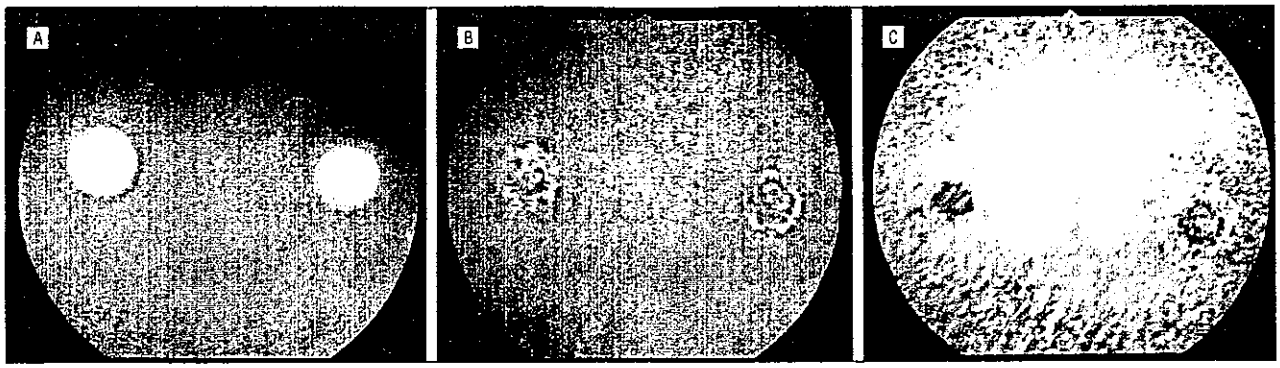

Figure 1. Fundus photography. Three applications of transpupillary thermotherapy (TTT), using a spot size of 1.2 mm, were applied with slight overlap between 2 marker laser burns. No visible change to the retina was observed immediately after TTT (A) or at 4 weeks (B). Fluorescein angiography at 4 weeks did not show any hyperfluorescence or hypofluorescence (C).

chloride. Pupils were dilated with 0.5% tropicamide and 0.5% phenylephrine eye drops.

DETERMINATION OF LASER SETTINGS

We performed TTT using an 810-nm diode laser (OcuLight SLx; IRIS Medical Instruments, Inc, Mountain View, Calif) fitted with a TTT slitlamp adapter (SLALS; IRIS Medical Instruments Inc). In all laser applications, we used a Goldmann laser–coated contact lens (−67 diopters) with a magnification factor of approximately 1.247 in rabbits with 810-nm radiation calculated using values from Murphy and Howland[9] (Martin A. Mainster, PhD, MD, e-mail communication, May 27, 2002). First, we investigated the power required to create a funduscopically visible laser burn (threshold application). Using a spot size of 1.2 mm and a power setting of 75 mW or greater, a 60-second TTT application produced whitening of the retina. However, at a power of 50 mW with the same spot size and duration, no funduscopically visible change to the retina was observed (subthreshold application). We confirmed this subthreshold power setting in several different animals. Because 50 mW was the lowest power setting available on the laser system used, duration of treatment was changed to vary the total laser energy dose in the subthreshold applications in this study.

TTT PROCEDURE

Before TTT, 2 strong photocoagulative burns spaced slightly apart were created using the diode laser (size, 50 mm; power, 800 mW; duration, 0.2 seconds) in the posterior pole to serve as markers for use in subsequent histopathological processing. This was followed by 3 subthreshold applications (3 spots) of TTT placed in a slightly overlapping fashion between the 2 marker burns. Laser settings were as follows: diameter of 1.2 mm; power of 50 mW; and duration of 15, 30, or 60 seconds (with a fluence of 71, 143, or 286 J/cm^2, respectively). Color fundus photographs were taken immediately and at 4 weeks after treatment. Fluorescein angiography was performed at 4 weeks after treatment using a 1-mL injection of 10% fluorescein via the marginal ear vein. The animals were then killed, and the eyes were immediately removed for histopathological processing.

HISTOPATHOLOGICAL EXAMINATION

Freshly enucleated eyes were fixed in 2.5% glutaraldehyde and 2% formaldehyde for 48 hours. Sections of the posterior pole were stained with toluidine blue and examined by means of light microscopy. Samples postfixed in 1% buffered osmium tetroxide and stained with uranyl were examined by means of transmission electron microscopy (JEM-1010; JEOL, Ltd, Tokyo, Japan). For immunohistochemistry, sections were blocked and incubated with primary antibody against HSP60, HSP70, VCAM-1 (Santa Cruz Biotechnology, Inc, Santa Cruz, Calif), or TNF-α (Techne Corp, Minneapolis, Minn). Sections were then washed, incubated with secondary antibody using fluorescein isothiocyanate–conjugated anti-goat IgG (Vector Laboratories Inc, Burlingame, Calif), and viewed with a fluorescence microscope (Model BX50; Olympus Corp, Tokyo). Normal untreated eyes used for control samples were prepared in a similar manner for light and electron microscopy and for immunohistochemical staining.

RESULTS

FUNDUSCOPY AND FLUORESCEIN ANGIOGRAPHY

Ophthalmoscopically, no visible change to the retina was observed for all durations of treatment, immediately or at 4 weeks after TTT application (**Figure 1**A and B), with the exception of 1 eye with relatively heavy fundus pigmentation that underwent TTT for a duration of 60 seconds. Development of some pigmentary changes was observed by 4 weeks after TTT, and this eye was not included in the histopathological examination results. Regardless, fluorescein angiography performed at 4 weeks showed no hypofluorescence or hyperfluorescence in the area of TTT application in this eye or in any other eye (Figure 1C).

LIGHT MICROSCOPY

In comparison with control eyes (**Figure 2**A), disruption of the normal configuration of photoreceptor outer segments was observed at 4 weeks after TTT application, even with the shortest duration of treatment of 15 seconds (Figure 2B). This disruption was increasingly more pronounced at 30 and 60 seconds of treatment (Figure 2C and D), with observation of fewer cell nuclei and overall thinning of the outer nuclear layer. In addition, with progressive TTT duration, decreased density of nuclei in the outer nuclear layer and greater pigmentation in the retinal pigment epithelium (RPE) were noted. No changes were observed in the inner layers of the retina or in the choroid for any duration of treatment.

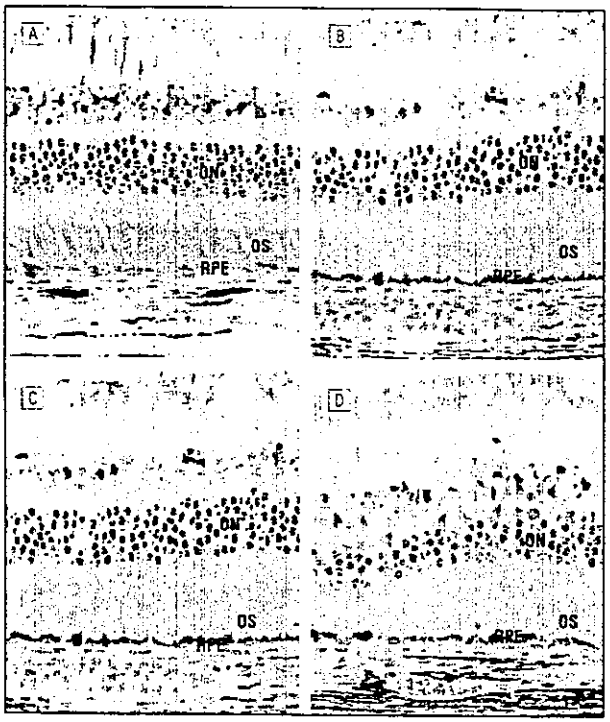

Figure 2. Light microscopy in an untreated control eye (A) and after transpupillary thermotherapy (TTT) (B-D) application. Even the shortest duration of 15 seconds caused disruption and thinning of the photoreceptor outer segment (OS) layer (B). This change was more pronounced with longer TTT durations of 30 seconds (C) and 60 seconds (D). With progressive TTT duration, decreased density of nuclei in the outer nuclear (ON) layer and greater pigmentation in the retinal pigment epithelium (RPE) were also noted (original magnification ×80).

TRANSMISSION ELECTRON MICROSCOPY

At low magnification, overall thinning of the photoreceptor layer with disruption of the outer and inner segments was observed, even at the shortest TTT duration of 15 seconds compared with controls (**Figure 3**A and B). With 60 seconds of treatment, the loss and disruption of photoreceptors were more pronounced (Figure 3C). Higher magnification showed vacuolization and distention of photoreceptor outer segments, with disruption of the lamellar structures of photoreceptors and apical microvilli of RPE cells at 15 (Figure 3D) and 30 seconds (not shown) of TTT duration. The normal basal infoldings of RPE cells appeared to be preserved. No changes were observed in Bruch's membrane or the anterior choroid for any duration of treatment.

IMMUNOHISTOCHEMISTRY

Results of tests for all antibodies were negative in all untreated controls (**Figure 4**A, D, F, and H). Staining for HSP60 was observed in the RPE and the inner segments of photoreceptors in eyes that received 30 seconds of TTT (Figure 4B), with the addition of staining for HSP60 observed in the photoreceptor outer segments at 60 seconds of treatment (Figure 4C). Staining for HSP70, TNF-α, and VCAM-1 was also observed in the RPE and the photoreceptor outer and inner segments for 30 and 60 seconds of TTT, with the staining appearing more pronounced for 60 seconds of TTT (Figure 4E, G, and I; data for 30 seconds of TTT are not shown). No staining for HSP60, HSP70, TNF-α, or VCAM-1 was observed in the inner layers of the retina, the outer nuclear layer, or the choroid for any duration of treatment.

COMMENT

Despite reports that TTT leads to decreased exudation in patients with CNV in age-related macular degeneration,[1,2] the mechanism of action of this therapy has yet to be delineated. Because little or no color change or burn is observed in the retina immediately after the subthreshold treatment involved in TTT, it is clear that the tissue effects differ from those of conventional laser photocoagulation. In addition, it is presumed that the higher wavelength of the infrared laser used (810 nm) would result in deeper tissue penetration and, consequently, less damage to the sensory retina when compared with photocoagulation using the argon or the dye laser. Thus, it has been suggested that TTT may be an ideal treatment for lesions involving the center of the fovea.

The present study shows that, even in the absence of funduscopic or angiographic evidence of alterations to the fundus, the outer retina and RPE are affected histologically by subthreshold TTT. Dose-dependent disruption of photoreceptor outer segments with loss of the outer nuclear layer was observed by means of light and electron microscopy. Furthermore, dose-dependent vacuolization of photoreceptor outer segments and RPE cells and disruption of RPE apical microvilli were also observed by means of electron microscopy. No adverse effect on the choroid was noted at the subthreshold energy levels used. Because normal pigmented rabbit eyes were used in these experiments, the results obtained cannot be directly extrapolated to the clinical setting in which TTT is used to treat a CNV lesion under the retina. Such lesions are usually in association with subretinal fluid, and this may serve to insulate the retina to some degree against heat absorption during TTT application. However, in eyes with CNV in which there is little associated subretinal fluid, our findings certainly highlight the need to consider decreasing power settings.

Previous histological studies of TTT have involved threshold settings to photocoagulate choroidal tumors.[7-9] However, 1 study examined subthreshold TTT to the normal macula in a human eye with choroidal melanoma that subsequently underwent enucleation.[10] That study reported abnormal cytopolasmic lipofuscin and melanofuscin granules in RPE cells and disruption of photoreceptor outer segments, with no changes observed in the choroid. Aside from the RPE granules, these findings are in agreement with what we observed in rabbit eyes.

Interpretation of our results must be tempered by differences in the refractive error and structure of rabbit vs human eyes. The irradiance (power/area) achieved using the same power, spot size, and contact lens will be lower in rabbit eyes than in human eyes.[6,11,12] For example, using the Goldmann lens and 810-nm radiation, the magnification factor is 1.247 in rabbits but only 1.08 in human eyes.[13] This results in an approximately 33% higher irradiance in human eyes than in rabbit eyes. There-

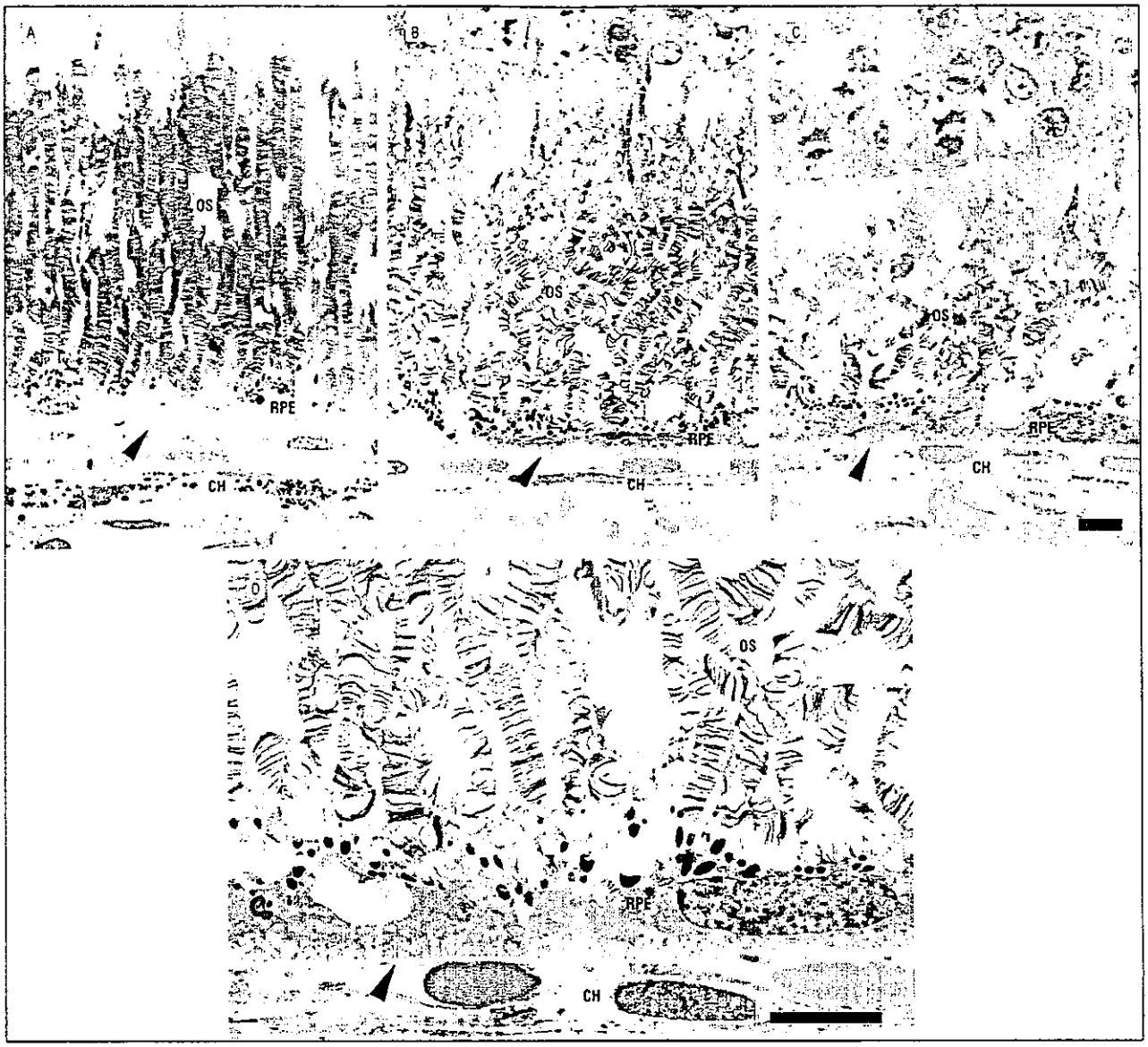

Figure 3. Transmission electron microscopy at low magnification in an untreated control eye (A) and after transpupillary thermotherapy (TTT) (B-D). After TTT duration of 15 seconds, overall thinning of the photoreceptor layer with disruption of the inner and outer segments (OS) of photoreceptor cells are observed (B). After TTT duration of 60 seconds, photoreceptor disruption is more pronounced (C) (original magnification for A, B, and C, ×2400; bar indicates 5 mm). At higher magnification, after TTT duration of 15 seconds, vacuolization and distention of photoreceptor outer segments are noted, with disruption of lamellar structures. The apical microvilli of retinal pigment epithelial (RPE) cells are also disrupted, although the normal basal infoldings are preserved (D) (original magnification ×5000; bar indicates 5 mm). Bruch's membrane (arrowheads) and the anterior choroid (CH) appear unaltered at all durations of TTT.

fore, one would expect the tissue effects observed in rabbits to be more pronounced in human eyes using identical laser settings.

The mechanism of action in the treatment of CNV using TTT is currently unclear. The expression of HSPs are known to be induced by heat and other pathologic stresses,[14-17] and recent studies have suggested that HSPs may play a major role in the effect of TTT.[4,5] Heat shock proteins are believed to act as molecular chaperones, theoretically allowing cells to adapt to unfavorable changes in their environment.[18-22] Heat shock proteins are also known to induce apoptosis, and therefore this may also contribute to the cellular alterations observed after TTT.[4,5,23] We examined the expression of HSP60 and HSP70 by immunohistochemistry after TTT in rabbit eyes and found both proteins to have a dose-dependent expression in the RPE and outer retina. In contrast, Desmettre and colleagues[5] reported the presence of HSP70 expression 24 hours after TTT in rabbits in choroidal cells, including capillary endothelial cells, but not in the retina. Expression of other proteins was not examined in that study. The fact that we assessed protein expression at 4 weeks after TTT may account for the difference in results between the study by Desmettre et al and our study. Expression of HSP has been shown to be induced within several hours after hyperthermia and to revert to control levels within 48 hours.[14,15] Expression of HSP60 and HSP70 at 4 weeks after TTT may therefore be the result of molecular interactions other than those induced by transient hyperthermia.

Indeed, HSPs have also been implicated in the downregulation of inflammatory cytokines such as TNF-α, in-

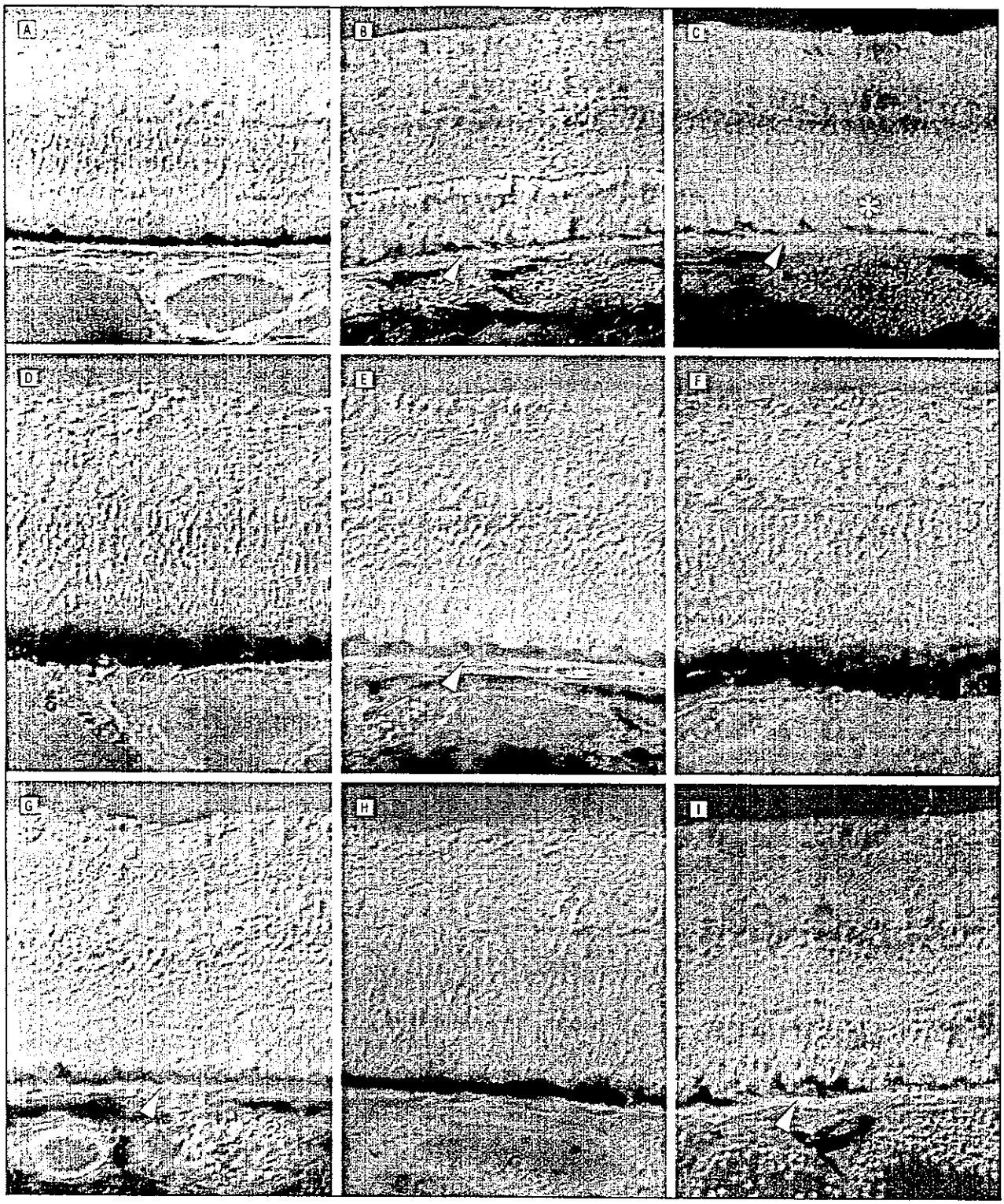

Figure 4. Results of immunohistochemistry in untreated control eyes showed no staining for heat shock protein 60 (HSP60) (A), HSP70 (D), tumor necrosis factor α (TNF-α) (F), or vascular cell adhesion molecule 1 (VCAM-1) (H). After transpupillary thermotherapy (TTT) duration of 30 seconds, HSP60 staining was present in the retinal pigment epithelium (RPE) (arrowhead) and inner segments of photoreceptor cells (asterisk) (B). After TTT duration of 60 seconds, HSP60 staining was observed in the inner and outer segments of photoreceptor cells (asterisk) and in the RPE (arrowhead) (C). After TTT duration of 60 seconds, staining for HSP70 (E), TNF-α (G), and VCAM-1 (I) were also observed in photoreceptor cells (asterisk) and in the RPE (arrowhead) in a similar dose-dependent manner as for HSP60. No staining for HSP60, HSP70, TNF-α, or VCAM-1 was observed in the inner layers of the retina, the outer nuclear layer, or the choroid for any TTT duration.

terleukin 1, and interleukin 6, and some of these same inflammatory cytokines have been shown to enhance HSP expression in an apparent cross-regulatory function.[24-30] In addition, HSP60 and HSP70 have each been shown to induce expression of intracellular adhesion molecule 1 and VCAM-1,[31,32] and one might speculate that

the long-term clinical effects of TTT are related to such adhesion molecule expression in the vessels of CNV lesions. In the present study, dose-dependent expression of TNF-α and VCAM-1 were also observed by means of immunohistochemical staining in the RPE and photoreceptors 4 weeks after TTT. Although these data suggest that the tissue effects of TTT involve the late expression of HSPs, TNF-α, and VCAM-1 in normal rabbit eyes, further experiments are clearly required to determine how such protein expression might lead to decreased exudation in eyes with CNV.

CONCLUSIONS

Subthreshold TTT in normal pigmented rabbit eyes produced alterations to the photoreceptor outer segments and RPE cells when assessed at 4 weeks after treatment. These alterations were accompanied by expression of HSP60, HSP70, TNF-α, and VCAM-1 within the outer retina and RPE. All changes were dose dependent and suggest that expression of HSPs, cytokines, and cell adhesion molecules may contribute to a delayed tissue response to subthreshold TTT.

Submitted for publication October 22, 2002; final revision received January 23, 2004; accepted March 26, 2004.

The authors thank Martin A. Mainster, PhD, MD, for his generous advice regarding lens image magnification in the rabbit eye, and also Minoru Fukuda and Nobuko Takahashi for their technical assistance.

Correspondence: Annabelle A. Okada, MD, Department of Ophthalmology, Kyorin University School of Medicine, 6-20-2 Shinkawa, Mitaka-shi, Tokyo 181-8611, Japan (aokada@po.iijnet.or.jp).

REFERENCES

1. Reichel E, Berrocal AM, Ip M, et al. Transpupillary thermotherapy of occult subfoveal choroidal neovascularization in patients with age-related macular degeneration. *Ophthalmology*. 1999;106:1908-1914.
2. Newsom RS, McAllister JC, Saeed M, McHugh JD. Transpupillary thermotherapy (TTT) for the treatment of choroidal neovascularisation [published correction appears in *Br J Ophthalmol*. 2001;85:505]. *Br J Ophthalmol*. 2001;85:173-178.
3. Ritchie KP, Keller BM, Syed KM, Lepock JR. Hyperthermia (heat-shock)–induced protein denaturation in liver, muscle and lens tissue as determined by differential scanning calorimetry. *Int J Hyperthermia*. 1994;10:605-618.
4. Mainster MA, Reichel E. Transpupillary thermotherapy for age-related macular degeneration: long-pulse photocoagulation, apoptosis, and heat shock proteins. *Ophthalmic Surg Lasers*. 2000;31:359-373.
5. Desmettre T, Maurage CA, Mordon S. Heat shock protein hyperexpression on chorioretinal layers after transpupillary thermotherapy. *Invest Ophthalmol Vis Sci*. 2001;42:2976-2980.
6. Murphy CJ, Howland HC. The optics of comparative ophthalmoscopy. *Vision Res*. 1987;27:599-607.
7. Journee-de Korver JG, Oosterhuis JA, de Wolff-Rouendaal D, Kemme H. Histopathological findings in human choroidal melanomas after transpupillary thermotherapy. *Br J Ophthalmol*. 1997;81:234-239.
8. Diaz CE, Capone A Jr, Grossniklaus HE. Clinicopathologic findings in recurrent choroidal melanoma after transpupillary thermotherapy. *Ophthalmology*. 1998;105:1419-1424.
9. Schurmans LR, Blom DJ, De Waard-Siebinga I, Keunen JE, Prause JU, Jager MJ. Effects of transpupillary thermotherapy on immunological parameters and apoptosis in a case of primary uveal melanoma. *Melanoma Res*. 1999;9:297-302.
10. Robertson DM, Salomao DR. The effect of transpupillary thermotherapy on the human macula. *Arch Ophthalmol*. 2002;120:652-656.
11. Hughes A. A schematic eye for the rabbit. *Vision Res*. 1972;12:123-138.
12. Pak MA. Ocular refraction and visual contrast sensitivity of the rabbit, determined by the VECP. *Vision Res*. 1984;24:341-345.
13. Mainster MA, Reichel E, Harrington PG, et al. Ophthalmoscopic contact lenses for transpupillary thermotherapy. *Semin Ophthalmol*. 2001;16:60-65.
14. D'Souza CA, Rush SJ, Brown IR. Effect of hyperthermia on the transcription rate of heat-shock genes in the rabbit cerebellum and retina assayed by nuclear runons. *J Neurosci Res*. 1998;52:538-548.
15. Tytell M, Barbe MF, Brown IR. Induction of heat shock (stress) protein 70 and its mRNA in the normal and light-damaged rat retina after whole body hyperthermia. *J Neurosci Res*. 1994;38:19-31.
16. Masing TE, Rush SJ, Brown IR. Induction of a heat shock gene (*hsp70*) in rabbit retinal ganglion cells detected by in situ hybridization with plastic-embedded tissue. *Neurochem Res*. 1990;15:1229-1235.
17. Yamaguchi K, Gaur VP, Tytell M, Hollman CR, Turner JE. Ocular distribution of 70-kDa heat-shock protein in rats with normal and dystrophic retinas. *Cell Tissue Res*. 1991;264:497-506.
18. Jaattela M. Heat shock proteins as cellular lifeguards. *Ann Med*. 1999;31:261-271.
19. Moseley PL. Heat shock proteins and the inflammatory response. *Ann N Y Acad Sci*. 1998;856:206-213.
20. Ohtsuka K, Laszlo A. The relationship between hsp 70 localization and heat resistance. *Exp Cell Res*. 1992;202:507-518.
21. Wakakura M, Kennedy PG, Foulds WS, Clements GB. Stress proteins accumulate in cultured retinal glial cells during herpes simplex viral infection. *Exp Eye Res*. 1987;45:557-567.
22. Tytell M, Barbe MF, Gower DJ. Photoreceptor protection from light damage by hyperthermia. *Prog Clin Biol Res*. 1989;314:523-538.
23. Mailhos C, Howard MK, Latchman DS. Heat shock protects neuronal cells from programmed cell death by apoptosis. *Neuroscience*. 1993;55:621-627.
24. Hall TJ. Role of hsp70 in cytokine production. *Experientia*. 1994;50(11-12):1048-1053.
25. Polla BS, Cossaizza A. Stress proteins in inflammation. In: Feige U, Morimoto RI, Yahara I, Polla B, eds. *Stress-Inducible Cellular Responses*. Basel, Switzerland: Birkhaeuser Verlag; 1996:375-391.
26. Jacquier-Sarlin MR, Fuller K, Dinh-Xuan AT, Richard MJ, Polla BS. Protective effects of hsp70 in inflammation. *Experientia*. 1994;50(11-12):1031-1038.
27. D'Souza SD, Antel JP, Freedman MS. Cytokine induction of heat shock protein expression in human oligodendrocytes: an interleukin-1–mediated mechanism. *J Neuroimmunol*. 1994;50:17-24.
28. Jiang Q, Detolla L, Singh IS, et al. Exposure to febrile temperature upregulates expression of pyrogenic cytokines in endotoxin-challenged mice. *Am J Physiol*. 1999;276(6, pt 2):R1653-R1660.
29. Bajramovic JJ, Bsibsi M, Geutskens SB, et al. Differential expression of stress proteins in human adult astrocytes in response to cytokines. *J Neuroimmunol*. 2000;106:14-22.
30. Wong HR. Potential protective role of the heat shock response in sepsis. *New Horiz*. 1998;6:194-200.
31. Galdiero M, De l'ero GC, Marcatili A. Cytokine and adhesion molecule expression in human monocytes and endothelial cells stimulated with bacterial heat shock proteins. *Infect Immun*. 1997;65:699-707.
32. Quarmby S, Kumar P, Kumar S. Radiation-induced normal tissue injury: role of adhesion molecules in leukocyte-endothelial cell interactions. *Int J Cancer*. 1999;82:385-395.